AUT Journal of Mechanical Engineering

AUT J. Mech. Eng., 5(4) (2021) 535-552
DOI: 10.22060/ajme.2021.18820.5922

Buckling Analysis of Stiffened Cross-Ply Laminated Conical Shells under Axial Compression Using Generalized Differential Quadrature Method

MM. A. Kouchakzadeh [1]*, P. Gholami [1], M. Shakouri [2], M. Noghabi [3]

[1] Department of Aerospace Engineering, Sharif University of Technology, Tehran, Iran
[2] Department of Aerospace Engineering, Semnan University, Semnan, Iran
[3] Iran Space Institute, Tehran, Iran

ABSTRACT: This study aims to determine the global buckling load of stiffened composite conical shells under axial compression. Stringers stiffen the conical shells in longitudinal and rings in circumferential directions. The boundary conditions are assumed to be simply supported at both ends. At first, the equilibrium equations are obtained using the first-order shear deformation theory and the principle of minimum potential energy. Effects of stiffeners (longitudinal and circumferential directions) are considered using the smearing technique. The resulting equations are solved using the generalized differential quadrature method to obtain the critical buckling load. The acquired results are compared with the finite element method results and other researcher's results available in the literature, and good agreement is observed. The influence of the number of stiffeners and rings, length, radius, semi-vertex angle of the cone, and shear deformation on the shell's buckling behavior is studied. Finally, the optimum number of stiffeners (longitudinal and circumferential directions) to achieve the maximum global buckling load in a cross-ply composite conical shell with various stacking sequences for a specific weight and overall geometry is investigated.

Review History:

Received:Aug. 03, 2020
Revised: Dec. 29, 2020
Accepted: Dec. 30, 2020
Available Online: Jan. 01, 2021

Keywords:

Stiffened conical shell
Laminated composite shell
Buckling
First-order shear deformation theory
Generalized differential quadrature

1- Introduction

Buckling of cylindrical and conical shell structures is one of the most complicated phenomena in many engineering branches, such as mechanical and civil engineering. Because of their outstanding capability in bearing loads for their weights, the study on stability and buckling of shells subjected to compressive forces is of great interest.

Many researchers have studied the buckling of the isotropic and composite conical shell under various loading conditions. A simple formula was derived for long isotropic conical shells under axial compression with simply supported boundary conditions by Seide [1]. Singer [2] studied the buckling of unstiffened conical shells under external pressure based on the stability equations for thin conical shells derived by Seide. Morgan et al. [3], and Seide and Weingarten [4] studied the stability of unstiffened conical shell under axial compression and external pressure. Tani [5] studied the buckling of unstiffened conical shells in large deformation under combined thermal loading and uniform pressure using the finite difference method. Zhou and Liu [6] derived an analytical formula for buckling of an unstiffened shell under uniform external pressure. Sofiyev [6] presented an analytic formula for the buckling of an orthotropic conical shell with continuously varying thickness. Using Galerkin's method Sofiyev and Schnack [7] studied the buckling of cross-ply laminated orthotropic truncated circular conical thin shells subjected to uniform external pressure. Baruch et al. [8] studied buckling loads of axially compressed unstiffened conical shells with various boundary conditions using the Galerkin method. Tong and his co-workers [9-11] used numerical integration technique and multi-segment method to obtain linear buckling analysis of unstiffened orthotropic and cross-ply laminated conical shells under uniform pressure and axial compression with various boundary conditions. Castro et al. [12] presented semi-analytical models for the linear buckling analysis of unstiffened laminated composite cylinders and cones under axial, torsional, and pressure loads (individually or combined) with flexible boundary conditions. This study used both of the classical laminated shell theory and the first-order shear deformation theory to derive the buckling equations. Based on the first order shear deformation theory, the analytical solutions of buckling behavior of Functionally Graded Material (FGM) cylindrical shells under mechanical loads are studied by Khazaeinejad and Najafzadeh [13]. In this study, the critical buckling loads' dependence on the material properties' variations is investigated. Buckling of a truncated conical composite sandwich panel using first order shear deformation theory is investigated by Fard and Livani [14]. Boundary conditions of the panel were assumed to be simply supported or fully clamped and the loading was considered to be axial compression and external pressure. The results were compared with Finite Element (FE) results.

*Corresponding author's email: mak@sharif.edu

Sofiyev and Kuruoglu [15] by using the Galerkin method, studied the buckling analysis of non-homogeneous orthotropic truncated conical shells with simply supported boundary conditions. The conical shell was subjected to combined loading of axial compression and external pressure. They investigated the effects of cone semi-vertex angle and other geometrical parameters on the critical load. An analytical approach was used for buckling analysis of generally laminated conical shells with various types of boundary conditions, subjected to axial pressure by Sharghi et al [16]. They used classical shell theory along with trigonometric functions in circumferential and power series in longitudinal directions. A closed-form solution for buckling of heterogeneous orthotropic truncated conical shell under external pressure was obtained by Sofyev [17]. First order shear deformation theory is used in the theoretical model and partial differential equations were solved by Galerkin method. Demir et al. [18] studied critical buckling loads of truncated conical panels made of isotropic, laminated and FGM materials. This study is based on the Donnell's shell theory and governing differential equations for buckling of the panel were solved using the method of Discrete Singular Convolution (DSC). Talebitooti [19] presented an analytical method for the buckling analysis of composite sandwich conical shells with clamped ends under external pressure. By using the Galerkin method, the equations of buckling load were achieved, and finally, the results of the analytical method for the critical pressure were verified in comparison with the results of the Finite Element Method (FEM). Torsional buckling of generally laminated conical shell subjected to uniform torsion with simply supported boundary conditions was studied by Shakouri et al. [20]. In this study, by using the Ritz method, governing equations were solved and critical buckling loads are obtained. Hu and Chen [21] investigated buckling of laminated truncated conical shells subjected to external hydrostatic compression using FEM. Kazemi et al. [22] presented the buckling of truncated laminated conical shells with linearly variable thickness under axial compression. By applying power series method, governing equations were solved and the results has been verified in comparison with the results of Galerkin method.

Goldfeld [23] studied the elastic buckling of stiffened conical shells and investigated the stiffeners' influence on the buckling load. In this study, a smeared approach is used, and only global buckling behavior is considered. Spagnoli and Chryssanthopoulos [24, 25] studied the buckling and post-buckling of stiffened conical shells. The buckling of the stiffened conical shells under hydrostatic pressure was studied by Baruch and singer [26]. Weingarten [27] investigated the free vibration of a ring-stiffened simply supported conical shell using the Galerkin method. Ross et al. [28] presented a numerical (FEM) and an experimental investigation of vibration of ring-stiffened thin-walled conical shells under external pressure. Experimental and numerical results are in agreement. Farkas et al. [29] analyzed the optimum design of a ring-stiffened conical shell loaded by external pressure. By using the Galerkin method, Dung et al. [30] studied buckling of an eccentrically stiffened sandwich truncated conical shell with FGM coating and core layer. In this study, shells were reinforced by stringers and rings subjected to an axial compressive load and an external uniform pressure. Buckling of functionally graded truncated conical shell was investigated by Van Dung and Chan [31]. In this study, the conical shell was reinforced by orthogonal stringers and rings and subjected to axial compressive load and external uniform pressure. The partial differential equations are derived based on the First-order Shear Deformation Theory (FSDT) using the smeared stiffener technique and were solved using the Galerkin method. Chan et al. [32] studied mechanical and thermal buckling of functionally graded material truncated conical shells, subjected to thermal load and axial compressive load with simply supported boundary conditions. The conical shells in this study are stiffened by stringers and rings. The equilibrium equations are obtained using the first order shear deformation theory and the Galerkin method is applied to obtain the critical buckling load.

The Generalized Differential Quadrature (GDQ) method is a compelling method to solve various equations based on the Differential Quadrature Method (DQM). Its main applications in engineering are discussed in detail by Shu [33]. Wu and Chen [34] used the GDQ method to study the buckling analysis of a multilayer anisotropic conical shell. Results are validated using ABAQUS, and the convergence is very fast. Shakouri and Kouchakzadeh [35] investigated the effects of semi-vertex angles and meridional lengths on the buckling load of two joined isotropic conical shells under axial compression with simply supported boundary conditions. Abediokhchi et al. [36] studied the buckling of cross-ply laminated conical shell panels with simply supported boundary conditions at all edges and subjected to axial compression using the GDQ method. Ansari and Torabi [37] investigated the buckling analysis of axially compressed functionally graded conical panels using DQM within the FSDT. By employing DQM, the thermal environment's effect on the vibration of functionally graded truncated conical shell panels within the FSDT was examined by Jooybar et al. [38].

There are some studies on the buckling of truncated conical shells using the classical shell theory or first-order shear deformation theory. However, most previous investigations are concerned with unstiffened conical shells, and the buckling behavior of stiffened laminated conical shell needs to be further studied.

Using the GDQ method, this paper discusses the buckling of moderately thick truncated conical shells stiffened by stringer and ring with simply supported boundary conditions at both ends and subjected to axial compression. The smeared stiffeners technique establishes the general form for force and moment resultants of stiffened truncated conical shells. The governing equations are obtained using FSDT and the theorem of minimum potential energy. Using the GDQ method, the governing partial differential equations are transformed into a set of linear algebraic governing equations. Imposing the boundary conditions, the standard eigenvalue equation is formed, and critical buckling load is calculated. The results are validated with the available results in the literature,

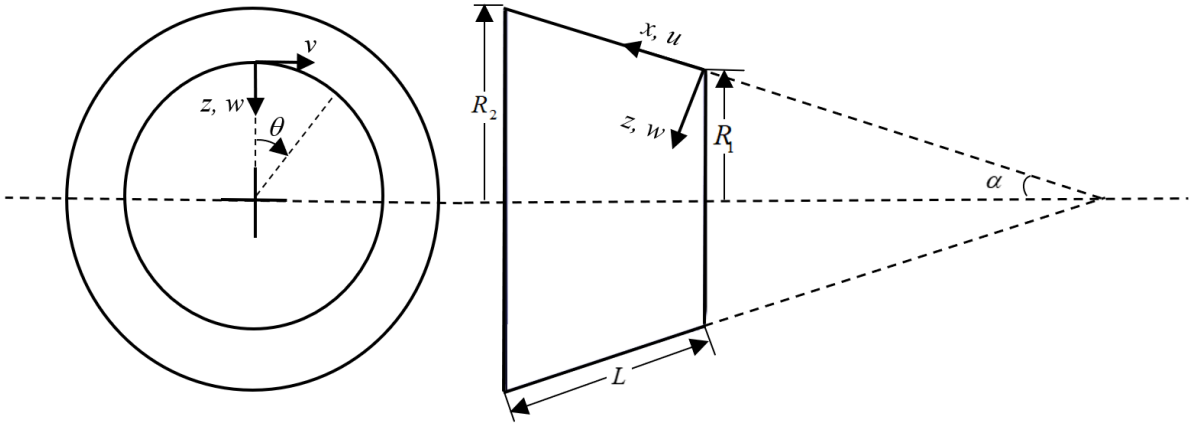

Fig. 1. The geometry of a conical shell

and good agreement is observed. The influences of various parameters such as are clarified in detail.

2- Theoretical Formulation

The geometry of a conical shell is shown in Fig. 1. The parameters R_1 and R_2 are respectively the radii of the cone at its small and large edges, α is the cone semi-vertex angle, and L is the length. The orthogonal coordinate system (x, θ, z) with its origin on the shell's reference surface is shown in Fig. 1. Displacements with reference to this orthogonal coordinate system are denoted by u, v, and w in the x, θ, and z directions, respectively. The radius of the cone at any point along its length is given by

$$R(x) = R_1 + x\sin\alpha \tag{1}$$

The equilibrium equations of motion in terms of the force and moment resultants are obtained using the principle of minimum potential energy. These equations can be written as [11]

$$\frac{\partial N_{xx}}{\partial x} + \frac{\sin(\alpha)}{R(x)}(N_{xx} - N_{\theta\theta}) + \frac{1}{R(x)}\frac{\partial N_{x\theta}}{\partial \theta} = 0,$$

$$\frac{\partial N_{x\theta}}{\partial x} + \frac{2\sin(\alpha)}{R(x)}N_{x\theta} + \frac{1}{R(x)}\frac{\partial N_{\theta\theta}}{\partial \theta} + Q_\theta\frac{\cos(\alpha)}{R(x)} = 0, \tag{2}$$

$$\frac{\partial Q_x}{\partial x} + \frac{1}{R(x)}\frac{\partial Q_\theta}{\partial \theta} + \frac{\sin(\alpha)}{R(x)}Q_x - \frac{\cos(\alpha)}{R(x)}N_{\theta\theta} + N_{x0}\frac{\partial^2 w}{\partial x^2} = 0,$$

$$\frac{\partial M_{xx}}{\partial x} + (M_{xx} - M_{\theta\theta})\frac{\sin(\alpha)}{R(x)} + \frac{1}{R(x)}\frac{\partial M_{x\theta}}{\partial \theta} - Q_x = 0,$$

$$\frac{\partial M_{x\theta}}{\partial x} + 2M_{x\theta}\frac{\sin(\alpha)}{R(x)} + \frac{1}{R(x)}\frac{\partial M_{\theta\theta}}{\partial \theta} - Q_\theta = 0.$$

in which N_{x0} is the pre-buckling load defined as

$$N_{x0} = \frac{-p}{2\pi R(x)\cos(\alpha)}. \tag{3}$$

The parameters N_i and M_i are the force and moment resultants defined as

$$\begin{Bmatrix} N_x \\ N_\theta \\ N_{x\theta} \end{Bmatrix} = \sum_{k=1}^{N}\int_{z_k}^{z_{k+1}} \begin{Bmatrix} \sigma_x \\ \sigma_\theta \\ \sigma_{x\theta} \end{Bmatrix}^{(k)} dz, \tag{4-a}$$

$$\begin{Bmatrix} M_x \\ M_\theta \\ M_{x\theta} \end{Bmatrix} = \sum_{k=1}^{N} \int_{z_k}^{z_{k+1}} \begin{Bmatrix} \sigma_x \\ \sigma_\theta \\ \sigma_{x\theta} \end{Bmatrix}^{(k)} z dz \,, \tag{4-b}$$

The transverse shear force resultant is

$$\begin{Bmatrix} Q_x \\ Q_\theta \end{Bmatrix} = K_s \sum_{k=1}^{N} \int_{z_k}^{z_{k+1}} \begin{Bmatrix} \sigma_{xz} \\ \sigma_{\theta z} \end{Bmatrix}^{(k)} dz \,. \tag{5}$$

where N is the total number of layers in the laminate

The stress–strain relations in the global coordinate system for the kth ply of the laminate are

$$\begin{Bmatrix} \sigma_x \\ \sigma_\theta \\ \sigma_{x\theta} \end{Bmatrix}^{(k)} = \begin{bmatrix} \bar{Q}_{11} & \bar{Q}_{12} & \bar{Q}_{16} \\ \bar{Q}_{12} & \bar{Q}_{22} & \bar{Q}_{26} \\ \bar{Q}_{16} & \bar{Q}_{26} & \bar{Q}_{66} \end{bmatrix}^{(k)} \times \left(\begin{Bmatrix} \varepsilon_x^0 \\ \varepsilon_\theta^0 \\ \gamma_{x\theta}^0 \end{Bmatrix} + z \begin{Bmatrix} \kappa_x \\ \kappa_\theta \\ \kappa_{x\theta} \end{Bmatrix} \right), \tag{6}$$

$$\begin{Bmatrix} \sigma_{\theta z} \\ \sigma_{xz} \end{Bmatrix}^{(k)} = \begin{bmatrix} \bar{Q}_{44} & \bar{Q}_{45} \\ \bar{Q}_{45} & \bar{Q}_{55} \end{bmatrix}^{(k)} \begin{Bmatrix} \gamma_{\theta z}^0 \\ \gamma_{xz}^0 \end{Bmatrix}.$$

where ε, γ, and κ are normal strain, shear strain, and curvature, respectively, while

$$\begin{aligned}
\bar{Q}_{11} &= Q_{11}\cos^4\phi + \\
&\quad 2(Q_{12}+2Q_{66})\sin^2\phi\cos^2\phi + Q_{22}\sin^4\phi, \\
\bar{Q}_{12} &= (Q_{11}+Q_{22}-4Q_{66})\sin^2\phi\cos^2\phi + \\
&\quad Q_{12}(\sin^4\phi+\cos^4\phi), \\
\bar{Q}_{22} &= Q_{11}\sin^4\theta + \\
&\quad 2(Q_{12}+2Q_{66})\sin^2\phi\cos^2\phi + Q_{22}\cos^4\phi, \\
\bar{Q}_{16} &= (Q_{11}-Q_{12}-2Q_{66})\sin\phi\cos^3\phi + \\
&\quad (Q_{12}-Q_{22}+2Q_{66})\sin^3\phi\cos\phi, \\
\bar{Q}_{26} &= (Q_{11}-Q_{12}-2Q_{66})\sin^3\phi\cos\phi + \\
&\quad (Q_{12}-Q_{22}+2Q_{66})\sin\phi\cos^3\phi, \\
\bar{Q}_{66} &= (Q_{11}+Q_{22}-2Q_{12}-2Q_{66})\sin^3\phi\cos\phi + \\
&\quad Q_{66}(\sin^4\phi+\cos^4\phi), \\
\bar{Q}_{44} &= Q_{44}\cos^2\phi + Q_{55}\sin^2\phi, \\
\bar{Q}_{45} &= (Q_{55}-Q_{44})\sin\phi\cos\phi, \\
\bar{Q}_{55} &= Q_{55}\cos^2\phi + Q_{44}\sin^2\phi.
\end{aligned} \tag{7}$$

where ϕ is the angular orientation of the fibers. The material constants Q_{ij} are defined as

$$\begin{aligned}
Q_{11} &= \frac{E_{11}}{1-\nu_{12}\nu_{21}}, & Q_{22} &= \frac{E_{22}}{1-\nu_{12}\nu_{21}}, & & \\
Q_{12} &= \frac{E_{11}\nu_{12}}{1-\nu_{12}\nu_{21}}, & Q_{21} &= \frac{E_{22}\nu_{21}}{1-\nu_{12}\nu_{21}}, & Q_{12} &= Q_{21}, \\
Q_{66} &= G_{12}, & Q_{44} &= G_{23}, & Q_{55} &= G_{13}.
\end{aligned} \tag{8}$$

in which, E_{11} and E_{22} are Young's moduli, G_{12}, G_{23}, G_{13} are the shear moduli, and ν_{12}, ν_{21} are the Poisson's ratios of the material.

According to FSDT representation of Donnell type [39] for conical shells, the mid-surface strains and curvature changes are expressed as

$$\begin{aligned}
\varepsilon_x^0 &= \frac{\partial u}{\partial x}, \\
\kappa_x &= \frac{\partial \psi_x}{\partial x}, \\
\varepsilon_\theta^0 &= \frac{1}{R(x)}\left(\frac{\partial v}{\partial \theta} + u_0\sin(\alpha) + w\cos(\alpha)\right), \\
\kappa_\theta &= \frac{1}{R(x)}\left(\frac{\partial \psi_\theta}{\partial \theta} + \psi_x\sin(\alpha)\right), \\
\gamma_{x\theta}^0 &= \frac{1}{R(x)}\left(\frac{\partial u}{\partial \theta} - v\sin(\alpha)\right) + \frac{\partial v_0}{\partial x}, \\
\kappa_{x\theta} &= \frac{1}{R(x)}\left(\frac{\partial \psi_x}{\partial \theta} - \psi_\theta\sin(\alpha)\right) + \frac{\partial \psi_\theta}{\partial x}. \\
\gamma_{\theta z}^0 &= \frac{1}{R(x)}\frac{\partial w}{\partial \theta} - \frac{v}{R(x)} + \psi_\theta, \\
\gamma_{xz}^0 &= \frac{\partial w}{\partial x} + \psi_x,
\end{aligned} \tag{9}$$

where ψ_x and ψ_θ are the rotations of a transverse normal about θ and x axes, respectively. By assumption of Classical Shell Theory (CST) for thin shells, the rotations are considered as

$$\psi_x = -\frac{\partial w}{\partial x}, \quad \psi_\theta = -\frac{\partial w}{\partial \theta}. \tag{10}$$

By substituting Eqs. (6) to (9) into Eqs. (4) and (5), the force, moment, and shear resultants can be obtained as

$$\begin{Bmatrix} N_x \\ N_\theta \\ N_{x\theta} \end{Bmatrix} = \begin{bmatrix} A_{11} & A_{12} & A_{16} \\ A_{21} & A_{22} & A_{26} \\ A_{61} & A_{62} & A_{66} \end{bmatrix} \begin{Bmatrix} \varepsilon_x^0 \\ \varepsilon_\theta^0 \\ \gamma_{x\theta}^0 \end{Bmatrix} + \begin{bmatrix} B_{11} & B_{12} & B_{16} \\ B_{21} & B_{22} & B_{26} \\ B_{61} & B_{62} & B_{66} \end{bmatrix} \begin{Bmatrix} \kappa_x \\ \kappa_\theta \\ \kappa_{x\theta} \end{Bmatrix}, \tag{11-a}$$

$$\begin{Bmatrix} M_x \\ M_\theta \\ M_{x\theta} \end{Bmatrix} = \begin{bmatrix} B_{11} & B_{12} & B_{16} \\ B_{21} & B_{22} & B_{26} \\ B_{61} & B_{62} & B_{66} \end{bmatrix} \begin{Bmatrix} \varepsilon_x^0 \\ \varepsilon_\theta^0 \\ \gamma_{x\theta}^0 \end{Bmatrix} + \begin{bmatrix} D_{11} & D_{12} & D_{16} \\ D_{21} & D_{22} & D_{26} \\ D_{61} & D_{62} & D_{66} \end{bmatrix} \begin{Bmatrix} \kappa_x \\ \kappa_\theta \\ \kappa_{x\theta} \end{Bmatrix}, \tag{11-b}$$

$$\begin{Bmatrix} Q_x \\ Q_\theta \end{Bmatrix} = K_s \begin{bmatrix} A_{55} & A_{54} \\ A_{45} & A_{44} \end{bmatrix} \begin{Bmatrix} \gamma_{xz}^0 \\ \gamma_{\theta z}^0 \end{Bmatrix}. \tag{11-c}$$

where A_{ij} , B_{ij} and D_{ij} are the extensional, coupling, and bending stiffnesses, respectively, which are defined as

$$(A_{ij}, B_{ij}, D_{ij}) = \int_{-h/2}^{h/2} \bar{Q}_{ij} (1, z, z^2) dz, \quad i, j = 1, 2, 6 \tag{12}$$

and A_{44}, $A_{45,}$ and A_{55} are

$$(A_{44}, B_{45}, D_{55}) = \int_{-h/2}^{h/2} \left(\bar{Q}_{44}, \bar{Q}_{45}, \bar{Q}_{55}\right) dz \tag{13}$$

The present work can be used for both internally and externally eccentric stiffeners in a general position. The shell is assumed to be closely stiffened. Therefore, there is no probable local buckling between stiffeners, and it is possible to "smear" the stiffeners [26], so the stress resultants and moment per unit length are given by

$$\begin{aligned} N_{ij} &= N_{ij}^{shell} + N_{ij}^{Stiff}, \\ M_{ij} &= M_{ij}^{shell} + M_{ij}^{Stiff}. \end{aligned} \tag{14}$$

where N_{ij}^{shell} and M_{ij}^{shell} are the stress resultants and moments per unit length of the shells' sheet. N_{ij}^{Stiff} and M_{ij}^{Stiff} are the stiffeners' contributions to the load-carrying capacity of the shell (per unit length). These contributions are based on the assumptions of Ref. [40]. Based on these assumptions, the internal forces and moments resultants, due to the stiffeners only, are created as functions of the strains and the curvatures of the reference surface in the direction of the stiffeners

$$\begin{bmatrix} N_{11} \\ N_{22} \\ N_{12} \\ M_{11} \\ M_{22} \\ (M_{12} + M_{21})/2 \end{bmatrix} = \begin{bmatrix} a_{11} & 0 & 0 & b_{11} & 0 & 0 \\ 0 & 0 & 0 & 0 & 0 & 0 \\ 0 & 0 & 0 & 0 & 0 & 0 \\ b_{11} & 0 & 0 & d_{11} & 0 & 0 \\ 0 & 0 & 0 & 0 & 0 & 0 \\ 0 & 0 & 0 & 0 & 0 & d_{66} \end{bmatrix} \begin{bmatrix} \varepsilon_1^0 \\ \varepsilon_2^0 \\ \gamma_{12}^0 \\ k_1 \\ k_2 \\ k_{12} \end{bmatrix} \tag{15}$$

where

$$\begin{aligned} a_{11} &= \frac{E_{st} A_{st}}{d}, \quad b_{11} = \frac{E_{st} A_{st} e}{d}, \\ d_{11} &= \frac{E_{st} I_{ost}}{d}, \quad d_{66} = (\frac{1}{4}) \frac{G_{st} I_{tst}}{d}. \end{aligned} \tag{16}$$

where G_{st} is the shear modulus of elasticity of the stiffener, A_{st} is the cross-sectional area of the stiffener, e is the distance of centroid of the stiffener cross-section from the reference surface, I_{ost} is the moment of inertia of the stiffener cross-section about the line of reference, and I_{tst} is the torsion constant of the stiffener cross-section. The parameter d is the distance between the stiffeners for a generally stiffened conical shell. It depends on the shell's coordinates $d(x, \theta)$ [40].

For optimization purposes, the geometrical characteristics of the cross-section of the stiffeners can be chosen to be a function of x and θ. Therefore, a_{11}, b_{11}, $d_{11,}$ and d_{66} are strong functions of the shell's coordinate. Hence, the contribution of stiffeners to stiffness matrices expressed in the basic coordinates system of the shell (x, θ) is given by [40]

$$\begin{aligned} A^{stiff} &= a_{11} J_1, \qquad B^{stiff} = b_{11} J_1, \\ \mathrm{D}^{stiff} &= d_{11} J_1 + d_{66} L_1. \end{aligned} \tag{17}$$

where

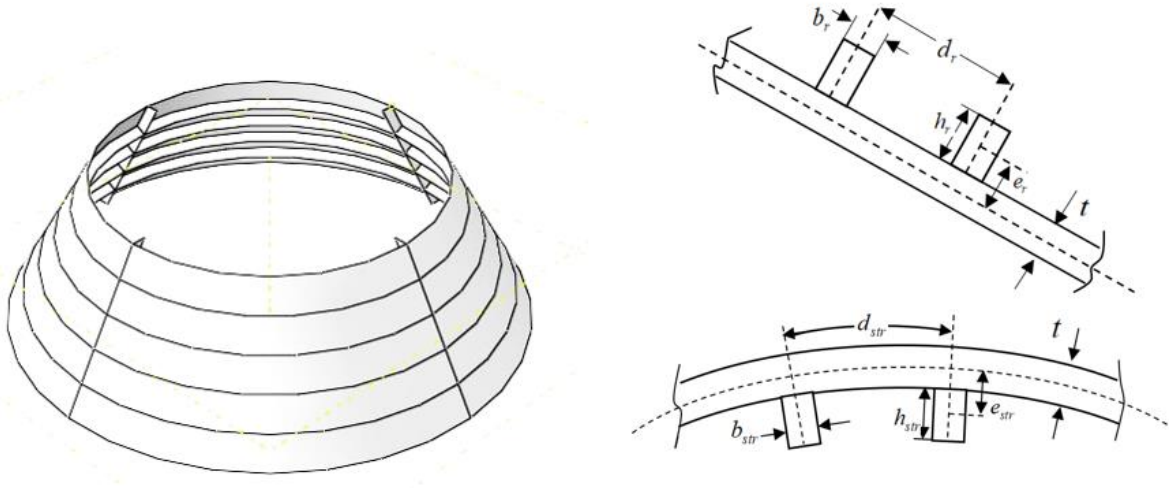

Fig. 2. The geometry of stiffened truncated conical shell structure

$$J_1=\begin{bmatrix} C^4 & C^2S^2 & C^3S \\ C^2S^2 & S^4 & CS^3 \\ C^3S & CS^3 & C^2S^2 \end{bmatrix}, \tag{18}$$

$$L_1=\begin{bmatrix} 4C^2S^2 & -4C^2S^2 & -2CS(C^2-S^2) \\ -4C^2S^2 & 4C^2S^2 & 2CS(C^2-S^2) \\ -2CS(C^2-S^2) & 2CS(C^2-S^2) & (C^2-S^2)^2 \end{bmatrix} \tag{19}$$

and $C=\cos[\beta(x,\theta)]$, $S=\sin[\beta(x,\theta)]$ and β is the angle of inclination of the stiffeners and is a function of x and θ, which depends on the chosen position of the stiffeners [40].

In this work, the inclination angle is considered to be $\beta=0$ and $\beta=\pi/2$ for the case of stringers and rings, respectively.

The distance between the stringers $d_{str}(x)$ is given by

$$d_{str}(x)=\frac{2\pi R(x)}{n_{str}} \tag{20}$$

and for the rings

$$d_r=\frac{L}{n_r} \tag{21}$$

where n_{str}, n_r are the number of stringer and ring, respectively.

Substituting Eqs. (9) and (11) into Eq. (2) leads to

$$\begin{bmatrix} L_{11} & L_{12} & L_{13} & L_{14} & L_{15} \\ L_{21} & L_{22} & L_{23} & L_{24} & L_{25} \\ L_{31} & L_{32} & L_{33} & L_{34} & L_{35} \\ L_{41} & L_{42} & L_{43} & L_{44} & L_{45} \\ L_{51} & L_{52} & L_{53} & L_{54} & L_{55} \end{bmatrix}\begin{bmatrix} u \\ v \\ w \\ \psi_x \\ \psi_\theta \end{bmatrix}=0 \tag{22}$$

where the linear partial differential operators L_{ij} are expressed in "Appendix A."

The *SS*3 or *SS*4 simply supported boundary conditions are considered at each edge of the conical shell as

$$\begin{aligned} &SS3: \quad v=w=\psi_\theta=N_{xx}=M_{xx}=0, \\ &SS4: \quad v=w=\psi_\theta=u=M_{xx}=0. \end{aligned} \tag{23}$$

The Generalized Differential Quadrature Method (GDQM) is especially appropriate for considering global characteristics such as buckling analyses [33, 36]. The numerical accuracy of the GDQM is outstanding, and its performance is reliable. The GDQM is developed based on the assumption that the partial derivation of a function with respect to a space variable of a given discrete point can be expressed as a weighted linear sum of the function values at all discrete points in the domain of that variable. Thus, applying the GDQ rules on the constitutive equation and boundary conditions, a set of simultaneous linear equations are obtained as

$$\begin{bmatrix} [S_{bb}] & [S_{bd}] \\ [S_{db}] & [S_{dd}] \end{bmatrix}\begin{Bmatrix} \{\Delta_b\} \\ \{\Delta_d\} \end{Bmatrix}=\lambda\begin{bmatrix} 0 & 0 \\ [B_{db}] & [B_{dd}] \end{bmatrix}\begin{Bmatrix} \{\Delta_b\} \\ \{\Delta_d\} \end{Bmatrix} \tag{24}$$

Table 1. Buckling ratio for anti-symmetric cross-ply laminate with SS4 boundary conditions ($R_1/t = 100$).

$\alpha(^o)$	L/R_0	0.2		0.5		1.0	
	N	Present study	Tong and Wang [11]	Present study	Tong and Wang [11]	Present study	Tong and Wang [11]
10	2	0.16612	0.1665	0.07908	0.07926	0.06975	0.0699
	4	0.22127	0.2218	0.10985	0.1101	0.10188	0.1021
	6	0.22530	0.2258	0.11165	0.1119	0.10678	0.1070
	16	0.22647	0.2270	0.11124	0.1115	0.11045	0.1107
30	2	0.18230	0.1827	0.08371	0.08389	0.09363	0.0938
	4	0.24367	0.2442	0.11037	0.1106	0.12236	0.1226
	6	0.24835	0.2489	0.11258	0.1128	0.12455	0.1248
	16	0.24986	0.2504	0.11246	0.1127	0.12445	0.1247
45	2	0.21275	0.2131	0.08691	0.08703	0.09369	0.0938
	4	0.28533	0.2858	0.11483	0.1150	0.12245	0.1226
	6	0.29071	0.2912	0.11713	0.1173	0.12465	0.1248
	16	0.29283	0.2933	0.11645	0.1166	0.12456	0.1247
60	2	0.28273	0.2831	0.09370	0.0938	0.07028	0.07034
	4	0.38156	0.3820	0.12248	0.1226	0.11180	0.1119
	6	0.38905	0.3895	0.12467	0.1248	0.11918	0.1193
	16	0.39263	0.3931	0.12469	0.1247	0.12448	0.1246

where λ is non-dimensional buckling load and Δ demonstrate the modal vector. The subscripts b and d represent the grid points at the boundary and remaining grid points, respectively. By eliminating Δ_b and then solving the generalized eigenvalue problem, buckling loads are determined [33].

3- Validation

To show the accuracy of the present analysis, two comparisons are made with the available results in the literature and the FEM. The initial comparison is made with Ref. [11] for an anti-symmetric cross-ply conical shell with *SS*4 boundary condition as shown in Table 1. This structure is an unstiffened conical shell.

The non-dimensional buckling load ratio ρ_0 is defined in the following form

$$\rho_0 = \frac{P_{cr}}{P_{cl}} \tag{25}$$

where P_{cl} is the value of critical buckling load for a conical shell with simply supported boundary condition suggested by Seide [1]

$$P_{cl} = \frac{2\pi E_{11} t^2 \cos^2(\alpha)}{\sqrt{3(1-\nu_{12}^2)}} \tag{26}$$

The coefficients in the constitutive equations for anti-symmetric cross-ply laminate are

$$\begin{aligned} &A_{11} = A_{22} = \frac{1}{2}(Q_{11}+Q_{22})t, \\ &A_{12} = Q_{12}\mathrm{t}, \qquad A_{66} = Q_{66}t, \\ &B_{11} = -B_{22} = \pm\frac{1}{4N}(Q_{11}-Q_{22})t^2, \\ &B_{12} = 0, \qquad B_{66} = 0, \\ &D_{11} = D_{22} = \frac{1}{24}(Q_{11}+Q_{22})t^3, \\ &D_{12} = \frac{1}{12}Q_{12}t^3, \qquad D_{66} = 0. \end{aligned} \tag{27}$$

The material of lamina is assumed to be graphite/epoxy

Table 2. Buckling ratio for various semi-vertex angles for SS4 boundary conditions ($R_1/h = 20$, $L/R_1 = 2$)

$\alpha(^o)$	GDQ	FEM
5	0.1861	0.1889
10	0.1839	0.1871
20	0.1664	0.1691
30	0.1423	0.1453
40	0.1160	0.1186
50	0.0810	0.0833
60	0.0481	0.0497
70	0.0218	0.0225
80	0.0109	0.0113

with the following material properties [11]

$$\begin{aligned} &E_{22} = E_{33} = E_{11}/40, \\ &G_{12} = G_{13} = 0.6E_{22}, \\ &G_{23} = 0.5E_{22}, \quad \nu_{12} = 0.25 \end{aligned} \tag{28}$$

Table 2 presents the comparison of this study's results with the FEM for cross-ply laminated conical shells which $R_1/t = 20$ and $L/R_1 = 2$. The FE analysis is performed using ABAQUS software with S4R shell element with *SS*4 simply-supported boundary conditions at both ends. Axial compression is applied, the convergence of the results for different element numbers is checked, and linear buckling for various semi-vertex angles is investigated. As shown in Table 2, a very good agreement is observable between the FEM results and the estimated buckling load, using the proposed model, which shows that the model is performing successfully.

For upcoming results, the following non-dimensional buckling load ratio are considered

$$\rho_1 = \frac{P_{cr}}{P_{cyl}} \tag{29}$$

where P_{cr} is the buckling load obtained, and P_{cyl} is the classical value of the buckling load for a long cylindrical shell with simply supported boundary conditions

$$P_{cyl} = \frac{2\pi E_{11} t^2}{\sqrt{3(1-\nu_{12}^2)}} \tag{30}$$

4- Numerical Results

4- 1- Effect of semi-vertex angle on the critical buckling load

The effects of semi-vertex angle and length to radius ratio on the buckling load of the conical shell stiffened with rings and stringers are studied in this section. For cross-ply laminated conical shells, the following properties are considered

$$\begin{aligned} &E_{22} = E_{33} = E_{11}/40, \quad G_{12} = G_{13} = 0.6E_{22}, \\ &G_{23} = 0.5E_{22}, \quad \nu_{12} = 0.25, \\ &R_1 = 0.2\,\text{m}, \quad R_1/t = 20, \\ &h_r = h_r = 0.01\,\text{m}, \quad b_{str} = b_r = 0.009\,\text{m} \end{aligned} \tag{31}$$

Fig. 3 shows the buckling load ratio of a simply supported (*SS*3), cross-ply laminated conical shell $[0/90/0]$ for various semi-vertex angles in different lengths to cone radii. The radius to thickness ratio is fixed at $R_1/t = 20$. It is seen that the buckling load decreases with increasing the semi-vertex angle. In addition, the buckling load is reduced in longer cones.

Fig. 4 shows the buckling load ratio for cross-ply laminated conical shells with various stacking sequences in which $R_1/t = 20$, $L/R_1 = 0.5$. As expected, the buckling load of conical shells with different stacking sequences decreases with increasing the semi-vertex angle.

4- 2- Effect of the shear deformation on the critical buckling loads

In this section, the critical buckling loads with first-order shear deformation theory and classical shell theory are studied. Table 3 summarizes the results of critical buckling load using FSDT and CST theories for the cross-ply laminated thin truncated conical shell $[0/90/0]$ with simply supported edges (*SS*3) for different cone radii to thickness (R_1/t) and constant semi-vertex angle ($\alpha = 30$). The mechanical properties of the material and geometrical parameters of the stiffeners are as in Eq. (31).

As expected, the critical buckling load ratios based on FSDT and CST are close in thin shells. The difference increase with shell thickness. For example, for a thick shell (i.e. $R_1/t = 5$), the CST buckling load ratio is 0.8158, which is about 4.08% greater than the result of FSDT.

4- 3- Design and optimization of laminated conical shells for buckling

One of this study's main objectives was to find the optimized number of stiffeners to bear maximum axial load in constant weight and geometric properties. To compare the results, an unstiffened cross-ply laminated conical shell is considered with $R_1/t = 20$, $L/R_1 = 2$, and $\alpha = 30$. The buckling load of this case is $P_{cr}^{unstiffened}$. Then, various numbers of stiffeners in both longitudinal and circumferential directions are considered to find the optimum number of stiffeners. The weight of the structure is assumed to be constant and geometrical properties of stiffeners are $h_{str} = h_r =$

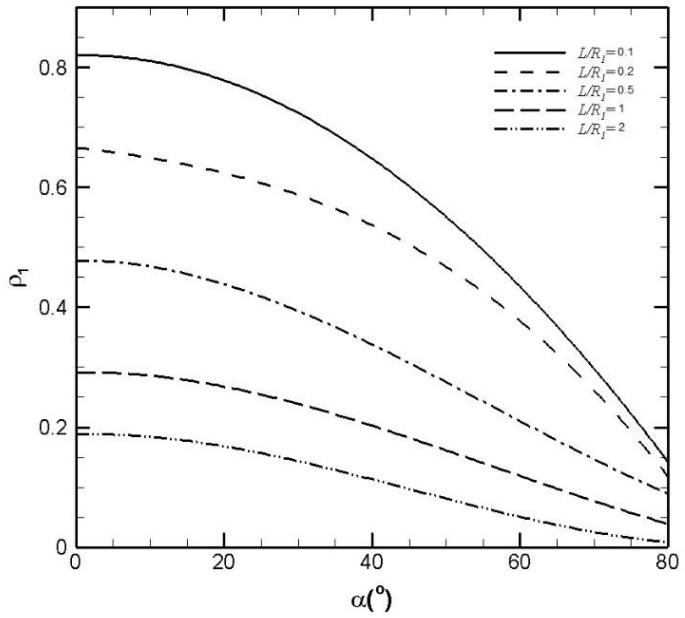

Fig. 3. Variation of buckling load ratio versus semi-vertex angle α, for SS3, cross-ply laminated conical shell $[0/90/0]$ **with** $R_1/t = 20$

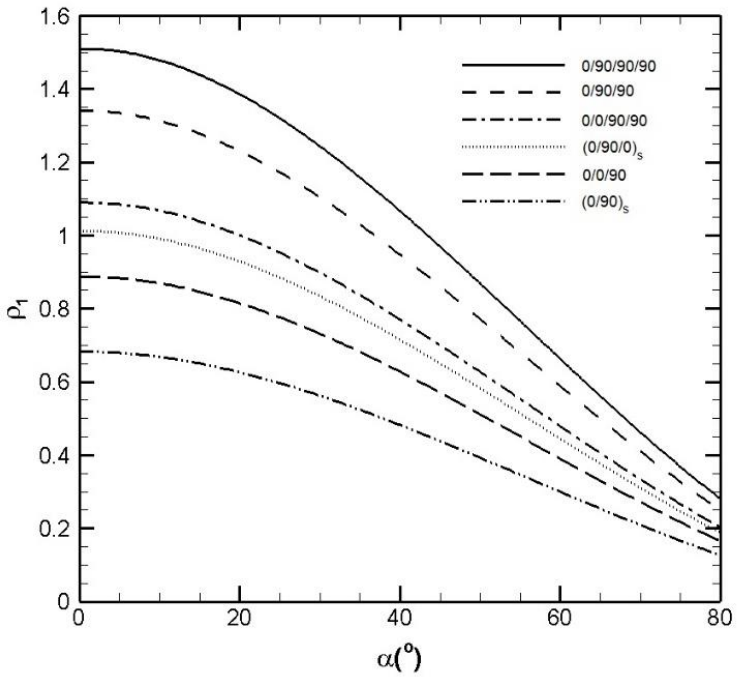

Fig. 4. Variation of buckling load ratio versus semi-vertex angle , for SS3, cross-ply laminated conical shells with various stacking sequences with $R_1/t = 20$, $L/R_1 = 0.5$.

Table 3. Comparisons of buckling load ratio ρ_1 of cross-ply laminated $[0/90/0]$ conical shell for SS3 boundary condition with CST and FSDT

R_1/t	Orthogonal ($n_s = n_r = 20$)		Orthogonal ($n_s = n_r = 30$)	
	CST	FSDT	CST	FSDT
5	0.8158	0.7838	0.9079	0.8659
10	0.3684	0.3615	0.4118	0.3597
20	0.1439	0.1424	0.1598	0.1563
50	0.0251	0.0250	0.0278	0.0276
100	0.0083	0.0083	0.0091	0.0090

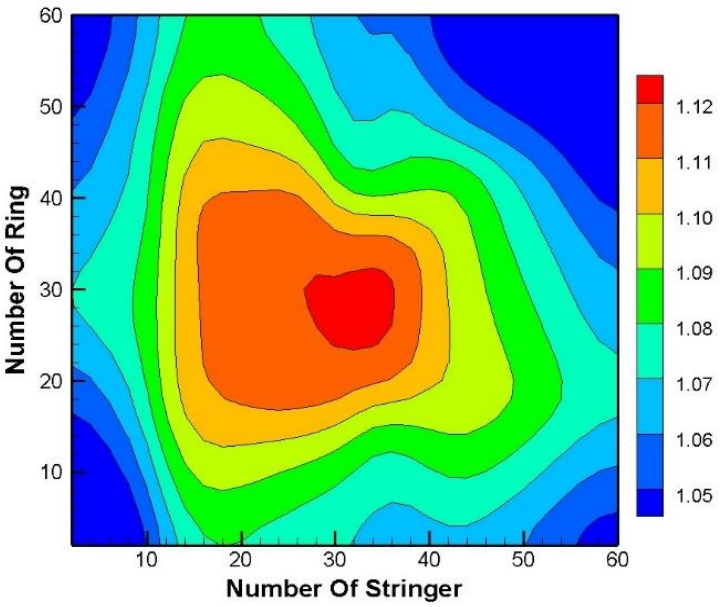

Fig. 5. Variation of buckling load ratio ρ_{cr}^{*} versus the number of stringers, for SS3, cross-ply laminated conical shell $[0/90/0]$ with $R_1/t = 20$, $L/R_1 = 2$ and $\alpha = 30$

0.01m, $b_{str} = b_r = 0.009$m. According to the Fig. 1, the weight of the conical shell is obtained as

$$M = V.\rho = \left[\frac{1}{3}\cdot\pi\cdot L\left(R_1^2 + R_1\cdot R_2 + R_2^2\right)\cos\alpha\right].\rho \quad (32)$$

Where V and ρ are the volume of the truncated cone and mean density of the cone, respectively. The weight of each stiffener is [41]

$$Weight_{stiff} = h_{str}\times b_{str}\times l\times\rho_{stiff} \quad (33)$$

So that l is the length of the stringer. The weight of the conical structure must be kept constant in the stiffened and unstiffened configurations. For this purpose, as the weight of the stiffeners increases, the thickness of the conical shell should decrease. Now, as the number (and weight) of stiffeners increases, the critical load values are calculated until the shell is not able to tolerate the load.

As already mentioned, in the present work, a smearing approach is adopted. Therefore, only global buckling behavior is considered. For a specific weight, Fig. 5 presents the effects of the number of stiffeners on the buckling ratio $\rho_{cr}^{*} = P_{cr}^{stiffened} / P_{cr}^{unstiffened}$ for cross-ply laminated conical shell [0/90/0]. The buckling load of the structures increases with the increase in the number of stiffeners. However, since the structure's weight is constant, the main shell's thickness decreases with an

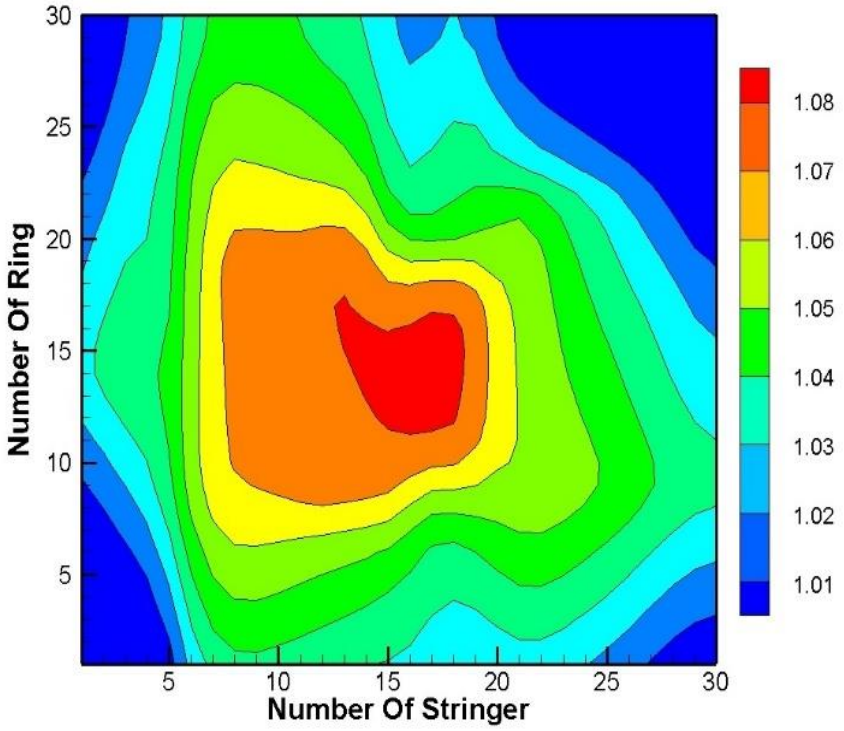

Fig. 6. Variation of buckling load ratio ρ_{cr}^{*} versus the number of stringers, for SS3, cross-ply laminated conical shell $[0/90]_s$ with $R_1/t = 20$, $L/R_1 = 2$ and $\alpha = 30$

increase in stiffeners' numbers, and an optimum condition occurs. The results show that the optimum numbers of stiffeners are $n_s = 33, n_r = 28$. In this case, the structure can bear the axial loads, which are 12 percent more than the unstiffened conical shell. In Fig. 6, the effects of stiffeners' number on the buckling load ratio for cross-ply laminated conical shell $[0/90]_s$ are shown. In this case, the optimum numbers of stiffeners are $n_s = 18, n_r = 14$, and the stiffened structure can tolerate 8 percent more axial load under the same conditions than an unstiffened structure.

5- Conclusion

The buckling of reinforced composite conical shells under axial compression is investigated by the generalized differential quadrature method. Shells are reinforced by stringers and rings, and the boundary conditions are assumed to be simply supported. The governing equations and boundary conditions are obtained using FSDT, smeared stiffener technique, and minimum potential energy principle. The results show that the buckling load of cross-ply laminated conical shell decreases with increasing the semi-vertex angles and length. The results of CST show lower accuracy for thick shells, and there is an optimum number of stiffeners to achieve the maximum buckling load in the composite conical shell for a specific weight.

Appendix A

$$
\begin{aligned}
L_{11} &= (A_{11}+\frac{E_{str}A_{str}}{d_{str}(x)})\frac{\partial^2}{\partial x^2}-\frac{E_{str}A_{str}}{d_{str}(x)^2}\frac{\partial}{\partial x}+\frac{\sin(\alpha)A_{12}}{R(x)}\frac{\partial}{\partial x}+\frac{A_{16}}{R(x)}\frac{\partial^2}{\partial x\,\partial\theta}\\
&+\frac{\sin(\alpha)}{R(x)}(A_{11}+\frac{E_{str}A_{str}}{d_{str}(x)}-A_{21})\frac{\partial}{\partial x}\\
&+\frac{\sin^2(\alpha)}{R(x)^2}(A_{12}-A_{22}-\frac{E_rA_r}{d_r})+\frac{\sin(\alpha)(A_{16}-A_{26})}{R(x)^2}\frac{\partial^2}{\partial x\,\partial\theta}+\frac{A_{61}}{R(x)}\frac{\partial^2}{\partial x\,\partial\theta}\\
&+\frac{\sin(\alpha)A_{62}}{R(x)^2}\frac{\partial}{\partial\theta}+\frac{A_{66}}{R(x)^2}\frac{\partial^2}{\partial\theta^2},\\
L_{12} &= A_{16}\frac{\partial^2}{\partial x^2}-\frac{\sin(\alpha)A_{16}}{R(x)}\frac{\partial}{\partial x}+\frac{A_{12}}{R(x)}\frac{\partial}{\partial\theta}+\frac{\sin(\alpha)}{R(x)^2}(A_{12}-A_{22}-\frac{E_rA_r}{d_r})\frac{\partial}{\partial\theta}\\
&+\frac{A_{16}-A_{26}}{R(x)^2}sin^2(\alpha)+\frac{\sin(\alpha)(A_{16}-A_{26})}{R(x)}\frac{\partial}{\partial x}-\frac{\sin(\alpha)A_{66}}{R(x)^2}\frac{\partial}{\partial\theta}\\
&+\frac{A_{66}}{R(x)}\frac{\partial^2}{\partial x\,\partial\theta}+\frac{A_{62}}{R(x)^2}\frac{\partial^2}{\partial\theta^2},\\
L_{13} &= \frac{\cos(\alpha)A_{12}}{R(x)}\frac{\partial}{\partial x}+\frac{\cos(\alpha)\sin(\alpha)}{R(x)^2}(A_{12}-A_{22}-\frac{E_rA_r}{d_r})+\frac{\cos(\alpha)A_{62}}{R(x)^2}\frac{\partial}{\partial\theta},\\
L_{14} &= (B_{11}+\frac{E_{str}A_{str}e_{str}}{d_{str}(x)})\frac{\partial^2}{\partial x^2}-\frac{E_{str}A_{str}e_{str}}{d_{str}(x)^2}\frac{\partial}{\partial x}+\frac{\sin(\alpha)B_{12}}{R(x)}\frac{\partial}{\partial x}+\frac{B_{16}}{R(x)}\frac{\partial^2}{\partial x\,\partial\theta}\\
&+\frac{\sin(\alpha)}{R(x)}(B_{11}+\frac{E_{str}A_{str}e_{str}}{d_{str}(x)}-B_{21})\frac{\partial}{\partial x}+\frac{\sin^2(\alpha)}{R(x)^2}(B_{12}-B_{22}-\frac{E_rA_re_r}{d_r})\\
&+\frac{\sin(\alpha)(B_{16}-B_{26})}{R(x)^2}\frac{\partial}{\partial\theta}+\frac{B_{61}}{R(x)}\frac{\partial^2}{\partial x\,\partial\theta}+\frac{\sin(\alpha)B_{62}}{R(x)^2}\frac{\partial}{\partial\theta}+\frac{B_{66}}{R(x)^2}\frac{\partial^2}{\partial\theta^2},\\
L_{15} &= \frac{B_{12}}{R(x)}\frac{\partial^2}{\partial x\,\partial\theta}-\frac{\sin(\alpha)B_{16}}{R(x)}\frac{\partial}{\partial x}+B_{16}\frac{\partial^2}{\partial x^2}+\frac{\sin(\alpha)}{R(x)^2}(B_{12}-B_{22}-\frac{E_rA_re_r}{d_r})\frac{\partial}{\partial\theta}\\
&-\frac{B_{16}-B_{26}}{R(x)^2}\sin^2(\alpha)+\frac{\sin(\alpha)(B_{16}-B_{26})}{R(x)}\frac{\partial}{\partial x}+\frac{B_{62}}{R(x)^2}\frac{\partial^2}{\partial\theta^2}-\frac{\sin(\alpha)B_{66}}{R(x)^2}\frac{\partial}{\partial\theta}\\
&+\frac{B_{66}}{R(x)}\frac{\partial^2}{\partial x\,\partial\theta}.
\end{aligned}
\tag{A.1}
$$

$$
\begin{aligned}
L_{21} &= \frac{A_{21}}{R(x)}\frac{\partial^2}{\partial x\,\partial\theta} + \frac{\sin(\alpha)}{R(x)^2}\left(A_{22} + \frac{E_r A_r}{d_r}\right)\frac{\partial}{\partial\theta} + \frac{A_{26}}{R(x)^2}\frac{\partial^2}{\partial\theta^2} + \frac{2\sin(\alpha)A_{61}}{R(x)}\frac{\partial}{\partial x} \\
&+ \frac{2\sin(\alpha)A_{62}}{R(x)^2} - \frac{2\sin(\alpha)A_{66}}{R(x)^2}\frac{\partial}{\partial\theta} + A_{61}\frac{\partial^2}{\partial x^2} + \frac{\sin(\alpha)A_{62}}{R(x)}\frac{\partial}{\partial x} \\
&- \frac{A_{66}}{R(x)}\frac{\partial^2}{\partial\theta\partial x}, \\
L_{22} &= \frac{1}{R(x)}\left(A_{22} + \frac{E_r A_r}{d_r}\right)\frac{\partial^2}{\partial\theta^2} - \frac{\sin(\alpha)A_{26}}{R(x)^2}\frac{\partial}{\partial\theta} + \frac{A_{26}}{R(x)}\frac{\partial^2}{\partial\theta\partial x} + \frac{2\sin(\alpha)A_{62}}{R(x)^2}\frac{\partial}{\partial\theta} \\
&- \frac{2\sin^2(\alpha)A_{66}}{R(x)^2} + \frac{2\sin(\alpha)A_{66}}{R(x)}\frac{\partial}{\partial x} + \frac{A_{62}}{R(x)}\frac{\partial^2}{\partial x\,\partial\theta} - \frac{\sin(\alpha)A_{66}}{R(x)}\frac{\partial}{\partial x} \\
&+ A_{66}\frac{\partial^2}{\partial x^2} - \frac{k_s\cos^2(\alpha)A_{44}}{R(x)^2}, \\
L_{23} &= \frac{\cos(\alpha)}{R(x)^2}\left(A_{22} + \frac{E_r A_r}{d_r}\right)\frac{\partial}{\partial\theta} + \frac{2A_{62}}{R^2(x)}\sin(\alpha)\cos(\alpha) + \frac{\cos(\alpha)A_{62}}{R(x)}\frac{\partial}{\partial x} \\
&+ \frac{k_s\cos(\alpha)A_{44}}{R(x)^2}\frac{\partial}{\partial\theta} + \frac{k_s\cos(\alpha)A_{45}}{R(x)}\frac{\partial}{\partial x}, \\
L_{24} &= \frac{B_{21}}{R(x)}\frac{\partial^2}{\partial\theta\partial x} + \frac{\sin(\alpha)}{R(x)^2}\left(\mathrm{B}_{22} + \frac{E_r A_r e_r}{d_r}\right)\frac{\partial}{\partial\theta} + \frac{B_{26}}{R(x)^2}\frac{\partial^2}{\partial\theta^2} + \frac{2\sin(\alpha)B_{61}}{R(x)}\frac{\partial}{\partial x} \\
&+ \frac{2\sin^2(\alpha)B_{62}}{R(x)^2} + \frac{2\sin(\alpha)B_{66}}{R(x)^2}\frac{\partial}{\partial\theta} + B_{61}\frac{\partial^2}{\partial x^2} + \frac{\sin(\alpha)B_{62}}{R(x)}\frac{\partial}{\partial x} \\
&+ \frac{B_{66}}{R(x)}\frac{\partial^2}{\partial\theta\partial x} + \frac{k_s\cos(\alpha)A_{45}}{R(x)}, \\
L_{25} &= \frac{1}{R(x)^2}\left(\mathrm{B}_{22} + \frac{E_r A_r e_r}{d_r}\right)\frac{\partial^2}{\partial\theta^2} - \frac{B_{26}\sin(\alpha)}{R(x)^2}\frac{\partial}{\partial\theta} + \frac{B_{26}}{R(x)}\frac{\partial^2}{\partial\theta\partial x} + \frac{2\sin(\alpha)B_{62}}{R(x)^2}\frac{\partial}{\partial\theta} \\
&- \frac{2B_{66}\sin^2(\alpha)}{R(x)^2} + \frac{2B_{66}\sin(\alpha)}{R(x)}\frac{\partial}{\partial x} + \frac{B_{62}}{R(x)}\frac{\partial^2}{\partial\theta\partial x} - \frac{B_{66}\sin(\alpha)}{R(x)}\frac{\partial}{\partial x} \\
&+ B_{66}\frac{\partial^2}{\partial x^2} + \frac{k_s\cos(\alpha)A_{44}}{R(x)}.
\end{aligned}
\tag{A.2}
$$

$$
\begin{aligned}
L_{31} &= -\frac{\cos(\alpha)A_{21}}{R(x)}\frac{\partial}{\partial x} - \frac{\sin(\alpha)\cos(\alpha)}{R(x)^2}(A_{22}+\frac{E_rA_r}{d_r}) - \frac{\cos(\alpha)A_{26}}{R(x)^2}\frac{\partial}{\partial\theta},\\
L_{32} &= -\frac{\cos(\alpha)}{R(x)^2}(A_{22}+\frac{E_rA_r}{d_r})\frac{\partial}{\partial\theta} + \frac{A_{26}}{R(x)^2}\sin(\alpha)\cos(\alpha) - \frac{\cos(\alpha)A_{26}}{R(x)}\frac{\partial}{\partial x}\\
&\quad - \frac{k_sA_{54}}{R(x)^2}\sin(\alpha)\cos(\alpha) - \frac{k_s\cos(\alpha)A_{54}}{R(x)^2}\frac{\partial}{\partial x} - \frac{k_s\cos(\alpha)A_{44}}{R(x)^2}\frac{\partial}{\partial\theta},\\
L_{33} &= -\frac{\cos^2(\alpha)}{R(x)^2}(A_{22}+\frac{E_rA_r}{d_r}) + \frac{k_s\sin(\alpha)A_{54}}{R(x)^2}\frac{\partial}{\partial\theta} + \frac{k_s\sin(\alpha)A_{55}}{R(x)}\frac{\partial}{\partial x}\\
&\quad + \frac{k_sA_{54}}{R(x)}\frac{\partial^2}{\partial x\,\partial\theta} + \frac{k_sA_{55}}{R(x)}\frac{\partial^2}{\partial x^2} + \frac{k_sA_{44}}{R(x)^2}\frac{\partial^2}{\partial\theta^2} + \frac{k_sA_{45}}{R(x)}\frac{\partial^2}{\partial x\,\partial\theta} + N_{x0}\frac{\partial^2}{\partial x^2},\\
L_{34} &= -\frac{\cos(\alpha)B_{21}}{R(x)}\frac{\partial}{\partial x} - \frac{\sin(\alpha)\cos(\alpha)}{R(x)^2}(B_{22}+\frac{E_rA_re_r}{d_r}) - \frac{\cos(\alpha)B_{26}}{R(x)^2}\frac{\partial}{\partial\theta}\\
&\quad + \frac{k_s\sin(\alpha)A_{55}}{R(x)} + k_sA_{55}\frac{\partial}{\partial x} + \frac{k_sA_{45}}{R(x)}\frac{\partial}{\partial\theta},\\
L_{35} &= -\frac{\cos(\alpha)}{R(x)}(B_{22}+\frac{E_rA_re_r}{d_r})\frac{\partial}{\partial\theta} + \frac{B_{26}}{R(x)^2}\sin(\alpha)\cos(\alpha) - \frac{\cos(\alpha)B_{26}}{R(x)}\frac{\partial}{\partial x}\\
&\quad + \frac{k_s\sin(\alpha)A_{54}}{R(x)} + k_sA_{54}\frac{\partial}{\partial x} + \frac{k_sA_{44}}{R(x)}\frac{\partial}{\partial\theta}.
\end{aligned}
\tag{A.3}
$$

$$
\begin{aligned}
L_{41} &= (B_{11}+\frac{E_{str}A_{str}e_{str}}{d_{str}(x)})\frac{\partial^2}{\partial x^2} - \frac{E_{str}A_{str}e_{str}}{d_{str}(x)^2}\frac{\partial}{\partial x} + \frac{\sin(\alpha)B_{12}}{R(x)}\frac{\partial}{\partial x} - \frac{B_{16}}{R(x)}\frac{\partial^2}{\partial x\,\partial\theta}\\
&\quad + \frac{\sin(\alpha)}{R(x)}(B_{11}+\frac{E_{str}A_{str}e_{str}}{d_{str}(x)}-B_{21})\frac{\partial}{\partial x} + \frac{\sin^2(\alpha)}{R(x)^2} + \frac{\sin(\alpha)(B_{16}-B_{26})}{R(x)^2}\frac{\partial}{\partial\theta}\\
&\quad + \frac{B_{61}}{R(x)}\frac{\partial^2}{\partial x\,\partial\theta} + \frac{\sin(\alpha)B_{62}}{R(x)^2}\frac{\partial}{\partial\theta} + \frac{B_{66}}{R(x)^2}\frac{\partial^2}{\partial\theta^2},\\
L_{42} &= B_{16}\frac{\partial^2}{\partial x^2} - \frac{\sin(\alpha)B_{16}}{R(x)}\frac{\partial}{\partial x} + \frac{B_{12}}{R(x)}\frac{\partial}{\partial x\,\partial\theta} + \frac{\sin(\alpha)}{R(x)^2}(B_{12}-B_{22}-\frac{E_rA_re_r}{d_r})\frac{\partial}{\partial\theta}\\
&\quad + \frac{B_{16}-B_{26}}{R(x)^2}\sin^2(\alpha) + \frac{\sin(\alpha)(B_{16}-B_{26})}{R(x)}\frac{\partial}{\partial x} - \frac{\sin(\alpha)B_{66}}{R(x)^2}\frac{\partial}{\partial\theta}\\
&\quad + \frac{B_{66}}{R(x)}\frac{\partial^2}{\partial x\,\partial\theta} + \frac{B_{62}}{R(x)^2}\frac{\partial^2}{\partial\theta^2} + \frac{k_s\cos(\alpha)A_{54}}{R(x)},
\end{aligned}
\tag{A.4}
$$

$$L_{43}=\frac{\cos(\alpha)B_{12}}{R(x)}\frac{\partial}{\partial x}+\frac{\cos(\alpha)\sin(\alpha)}{R(x)^2}(B_{12}-B_{22}-\frac{E_rA_re_r}{d_r})+\frac{\cos(\alpha)B_{62}}{R(x)^2}\frac{\partial}{\partial x}$$
$$-\frac{k_sA_{54}}{R(x)}\frac{\partial}{\partial\theta}-k_sA_{55}\frac{\partial}{\partial x},$$
(A.4)

$$L_{44}=(D_{11}+\frac{E_{str}I_{ostr}}{d_{str}(x)})\frac{\partial^2}{\partial x^2}-\frac{E_{str}I_{ostr}}{d_{str}(x)^2}\frac{\partial}{\partial x}+\frac{\sin(\alpha)D_{12}}{R(x)}\frac{\partial}{\partial x}+\frac{D_{16}}{R(x)}\frac{\partial^2}{\partial x\,\partial\theta}$$
$$+\frac{\sin(\alpha)}{R(x)}(D_{11}+\frac{E_{str}I_{ostr}}{d_{str}(x)}-D_{21})\frac{\partial}{\partial x}+\frac{\sin^2(\alpha)}{R(x)^2}(D_{12}-D_{22}-\frac{E_rI_{or}}{d_r})$$
$$+\frac{\sin(\alpha)(D_{16}-D_{26})}{R(x)^2}\frac{\partial}{\partial\theta}+\frac{B_{61}}{R(x)}\frac{\partial^2}{\partial x\,\partial\theta}+\frac{\sin(\alpha)B_{62}}{R(x)^2}\frac{\partial}{\partial\theta}+\frac{B_{66}}{R(x)^2}\frac{\partial^2}{\partial\theta^2}-K_SA_{55},$$

$$L_{45}=\frac{D_{12}}{R(x)}\frac{\partial^2}{\partial x\,\partial\theta}-\frac{\sin(\alpha)D_{16}}{R(x)}\frac{\partial}{\partial x}+D_{16}\frac{\partial^2}{\partial x^2}+\frac{\sin(\alpha)}{R(x)^2}(D_{12}-D_{22}-\frac{E_rI_{or}}{d_r})\frac{\partial}{\partial\theta}$$
$$-\frac{D_{16}-D_{26}}{R(x)^2}\sin^2(\alpha)+\frac{\sin(\alpha)(D_{16}-D_{26})}{R(x)}\frac{\partial}{\partial x}+\frac{B_{62}}{R(x)^2}\frac{\partial^2}{\partial\theta^2}-\frac{\sin(\alpha)B_{66}}{R(x)^2}\frac{\partial}{\partial\theta}$$
$$+\frac{B_{66}}{R(x)}\frac{\partial^2}{\partial x\,\partial\theta}-K_SA_{54}.$$

$$L_{51}=B_{61}\frac{\partial^2}{\partial x^2}+\frac{\sin(\alpha)B_{62}}{R(x)}\frac{\partial}{\partial x}+\frac{B_{66}}{R(x)}\frac{\partial^2}{\partial x\,\partial\theta}+\frac{2\sin(\alpha)B_{61}}{R(x)}\frac{\partial}{\partial x}+\frac{2\sin(\alpha)B_{62}}{R(x)^2}\frac{\partial}{\partial\theta}$$
$$+\frac{2\sin(\alpha)B_{66}}{R(x)^2}+\frac{B_{21}}{R(x)}\frac{\partial^2}{\partial x\,\partial\theta}-\frac{\sin(\alpha)}{R(x)^2}(\mathrm{B}_{22}+\frac{E_rA_re_r}{d_r})\frac{\partial}{\partial\theta}+\frac{B_{26}}{R(x)^2}\frac{\partial^2}{\partial\theta^2},$$

$$L_{52}=\frac{B_{62}}{R(x)}\frac{\partial^2}{\partial x\,\partial\theta}-\frac{\sin(\alpha)B_{66}}{R(x)}\frac{\partial}{\partial x}+\mathrm{B}_{66}\frac{\partial^2}{\partial x^2}+\frac{2\sin(\alpha)B_{62}}{R(x)^2}\frac{\partial}{\partial\theta}$$
$$-\frac{2\sin^2(\alpha)B_{66}}{R(x)^2}+\frac{2\sin(\alpha)B_{66}}{R(x)}\frac{\partial}{\partial x}+\frac{1}{R(x)^2}(\mathrm{B}_{22}+\frac{E_rA_re_r}{d_r})\frac{\partial^2}{\partial\theta^2}-\frac{\sin(\alpha)B_{26}}{R(x)^2}\frac{\partial}{\partial\theta}$$
$$+\frac{B_{26}}{R(x)}\frac{\partial^2}{\partial x\,\partial\theta}+\frac{k_s\cos(\alpha)A_{44}}{R(x)},$$

$$L_{53}=\frac{\cos(\alpha)B_{62}}{R(x)}\frac{\partial}{\partial x}+\frac{2B_{62}}{R(x)^2}\sin(\alpha)\cos(\alpha)+\frac{\cos(\alpha)}{R(x)^2}(\mathrm{B}_{22}+\frac{E_rA_re_r}{d_r})\frac{\partial}{\partial\theta}-\frac{k_sA_{44}}{R(x)}\frac{\partial}{\partial\theta}$$
$$-k_sA_{45}\frac{\partial}{\partial x},$$
(A.5)

$$L_{54}=D_{61}\frac{\partial^2}{\partial x^2}+\frac{\sin(\alpha)D_{62}}{R(x)}\frac{\partial}{\partial x}+\frac{D_{66}}{R(x)}\frac{\partial^2}{\partial x\,\partial\theta}+\frac{2\sin(\alpha)D_{61}}{R(x)}\frac{\partial}{\partial x}+\frac{2\sin^2(\alpha)D_{62}}{R(x)^2}$$

$$
\begin{aligned}
&+\frac{2\sin(\alpha)D_{66}}{R(x)^2}\frac{\partial}{\partial\theta}+\frac{D_{21}}{R(x)}\frac{\partial^2}{\partial x\,\partial\theta}+\frac{1}{R(x)^2}(\mathrm{D}_{22}+\frac{E_rI_{or}}{d_r})\frac{\partial}{\partial\theta}+\frac{D_{26}}{R(x)^2}\frac{\partial^2}{\partial\theta^2}\\
&-K_SA_{45},\\
L_{55}=&\frac{D_{62}}{R(x)}\frac{\partial^2}{\partial x\,\partial\theta}-\frac{D_{66}\sin(\alpha)}{R(x)}\frac{\partial}{\partial x}+D_{66}\frac{\partial^2}{\partial x^2}+\frac{2\sin(\alpha)D_{62}}{R(x)^2}\frac{\partial}{\partial\theta}\\
&-\frac{2D_{66}\sin^2(\alpha)}{R(x)^2}+\frac{2D_{66}\sin(\alpha)}{R(x)}\frac{\partial}{\partial x}+\frac{1}{R(x)^2}(\mathrm{D}_{22}+\frac{E_rI_{or}}{d_r})\frac{\partial^2}{\partial\theta^2}-\frac{D_{26}}{R(x)^2}\frac{\partial}{\partial\theta}\\
&+\frac{D_{26}}{R(x)}\frac{\partial^2}{\partial x\,\partial\theta}-K_SA_{54}.
\end{aligned}
\tag{A.5}
$$

The quantities A_{str}, A_r are the cross-section areas of stiffeners and I_{str}, I_r are the second moments of inertia of the stiffener cross-sections relative to the shell middle surface are defined

$$
\begin{aligned}
&A_{str}=b_{str}h_{str},\qquad A_r=b_rh_r,\\
&I_{str}=\frac{b_{str}h_{str}^3}{12}+A_{str}e_{str}^2,\qquad I_r=\frac{b_rh_r^3}{12}+A_re_r^2,
\end{aligned}
\tag{A.6}
$$

where n_{str}, n_r are the number of stringer and ring respectively; h_{str} and b_{str} are the thickness and width of stringer (x-direction); h_r and b_r are the thickness and width of the ring (θ-direction). Also, $d_{str}(x)$ and d_r are the distances between two stringers and two rings, respectively; and e_{str}, e_r present the eccentricities of stiffeners with respect to the middle surface of shell; the torsional rigidity of the stiffener cross-section is neglected ($I_{tst}=0$).

References

[1] P. Seide, Axisymmetrical buckling of circular cones under axial compression, Journal of Applied Mechanics, 23(1) (1956) 626-628.

[2] J. Singer, Buckling of circular conical shells under axisymmetrical external pressure, Journal of Mechanical Engineering Science, 3(4) (1961) 330-339.

[3] E. Morgan, P. Seide, V. Weingarten, Elastic stability of thin-walled cylindrical and conical shells under axial compression, AIAA Journal, 3(3) (1965) 500-505.

[4] P. Seide, V. Weingarten, Elastic stability of thin-walled cylindrical and conical shells under combined external pressure and axial compression, AIAA Journal, 3(5) (1965) 913-920.

[5] J. Tani, Buckling of truncated conical shells under combined pressure and heating, Journal of Thermal Stresses, 7(3-4) (1984) 307-316.

[6] A.H. Sofiyev, The buckling of an orthotropic composite truncated conical shell with continuously varying thickness subject to a time dependent external pressure, Composites Part B: Engineering, 34(3) (2003) 227-233.

[7] A. Sofiyev, E. Schnack, The buckling of cross-ply laminated non-homogeneous orthotropic composite conical thin shells under a dynamic external pressure, Acta mechanica, 162(1-4) (2003) 29-40.

[8] M. Baruch, O. Harari, J. Singer, Low Buckling Loads of Axially Compressed Conical Shells, Journal of Applied Mechanics, 37(2) (1970) 384.

[9] L. Tong, T.K. Wang, Buckling analysis of laminated composite conical shells, Composites Science and Technology, 47(1) (1993) 57-63.

[10] L. Tong, B. Tabarrok, T.K. Wang, Simples solutions for buckling of orthotropic conical shells, Solids Structures, 29(8) (1992) 933-946.

[11] L. Tong, T.K. Wang, Simple solutions for buckling of laminated conical shells, International Journal of

Mechanical Sciences, 34(2) (1992) 93-111.

[12] S.G. Castro, C. Mittelstedt, F.A. Monteiro, M.A. Arbelo, G. Ziegmann, R. Degenhardt, Linear buckling predictions of unstiffened laminated composite cylinders and cones under various loading and boundary conditions using semi-analytical models, Composite Structures, 118 (2014) 303-315.

[13] P. Khazaeinejad, M. Najafizadeh, Mechanical buckling of cylindrical shells with varying material properties, Proceedings of the Institution of Mechanical Engineers, Part C: Journal of Mechanical Engineering Science, 224(8) (2010) 1551-1557.

[14] K.M. Fard, M. Livani, The buckling of truncated conical sandwich panels under axial compression and external pressure, Proceedings of the Institution of Mechanical Engineers, Part C: Journal of Mechanical Engineering Science, 229(11) (2015) 1965-1978.

[15] A. Sofiyev, N. Kuruoglu, Buckling of non-homogeneous orthotropic conical shells subjected to combined load, Steel and Composite Structures, 19(1) (2015) 1-19.

[16] H. Sharghi, M. Shakouri, M. Kouchakzadeh, An analytical approach for buckling analysis of generally laminated conical shells under axial compression, Acta Mechanica, 227(4) (2016) 1181-1198.

[17] A. Sofiyev, Buckling of heterogeneous orthotropic composite conical shells under external pressures within the shear deformation theory, Composites Part B: Engineering, 84 (2016) 175-187.

[18] Ç. Demir, K. Mercan, Ö. Civalek, Determination of critical buckling loads of isotropic, FGM and laminated truncated conical panel, Composites Part B: Engineering, 94 (2016) 1-10.

[19] M. Talebitooti, Analytical and finite-element solutions for the buckling of composite sandwich conical shell with clamped ends under external pressure, Archive of Applied Mechanics, 87(1) (2017) 59-73.

[20] M. Shakouri, H. Sharghi, M. Kouchakzadeh, Torsional buckling of generally laminated conical shell, Meccanica, 52(4-5) (2017) 1051-1061.

[21] H.-T. Hu, H.-C. Chen, Buckling optimization of laminated truncated conical shells subjected to external hydrostatic compression, Composites Part B: Engineering, 135 (2018) 95-109.

[22] M. Kazemi, M. Kouchakzadeh, M. Shakouri, Stability analysis of generally laminated conical shells with variable thickness under axial compression, Mechanics of Advanced Materials and Structures, (2018) 1-14.

[23] Y. Goldfeld, Elastic buckling and imperfection sensitivity of generally stiffened conical shells, AIAA Journal, 45(3) (2007) 721-729.

[24] A. Spagnoli, M. Chryssanthopoulos, Elastic buckling and postbuckling behaviour of widely-stiffened conical shells under axial compression, Engineering Structures, 21(9) (1999) 845-855.

[25] A. Spagnoli, M.K. Chryssanthopoulos, Buckling design of stringer-stiffened conical shells in compression, Journal of Structural Engineering, 125(1) (1999) 40-48.

[26] M. Baruch, J. Singer, General instability of stiffened circular conical shells under hydrostatic pressure, Aeronautical Quarterly, 16(02) (1965) 187-204.

[27] V.I. Weingarten, Free vibrations of ring-stiffened conical shells, AIAA Journal, 3(8) (1965) 1475-1481.

[28] C. Ross, A. Little, L. Chasapides, J. Banks, D. Attanasio, The vibration of ring-stiffened prolate domes under external water pressure, Proceedings of the Institution of Mechanical Engineers, Part C: Journal of Mechanical Engineering Science, 217(2) (2003) 173-185.

[29] J. Farkas, K. Jármai, F. Orbán, Cost minimization of a ring-stiffened conical shell loaded by external pressure, Welding in the World, 52(5-6) (2008) 110-115.

[30] D. Dung, L. Hoa, B. Thuyet, N. Nga, Buckling analysis of functionally graded material (FGM) sandwich truncated conical shells reinforced by FGM stiffeners filled inside by elastic foundations, Applied Mathematics and Mechanics, 37(7) (2016) 879-902.

[31] D. Van Dung, D.Q. Chan, Analytical investigation on mechanical buckling of FGM truncated conical shells reinforced by orthogonal stiffeners based on FSDT, Compos. Struct., 159 (2017) 827-841.

[32] D.Q. Chan, D. Van Dung, L.K. Hoa, Thermal buckling analysis of stiffened FGM truncated conical shells resting on elastic foundations using FSDT, Acta Mechanica, 229(5) (2018).

[33] C. Shu, *Differential quadrature and its application in engineering*, Springer Science & Business Media, 2012.

[34] C.-P. Wu, C.-W. Chen, Elastic buckling of multilayered anisotropic conical shells, Journal of Aerospace Engineering, 14(1) (2001) 29-36.

[35] M. Shakouri, M.A. Kouchakzadeh, Stability analysis of joined isotropic conical shells under axial compression, Thin-Walled Structures, 72 (2013) 20-27.

[36] J. Abediokhchi, M. Kouchakzadeh, M. Shakouri, Buckling analysis of cross-ply laminated conical panels using GDQ method, Composites Part B: Engineering, 55 (2013) 440-446.

[37] R. Ansari, J. Torabi, Numerical study on the buckling and vibration of functionally graded carbon nanotube-reinforced composite conical shells under axial loading, Composites Part B: Engineering, 95 (2016) 196-208.

[38] N. Jooybar, P. Malekzadeh, A. Fiouz, M. Vaghefi, Thermal effect on free vibration of functionally graded truncated conical shell panels, Thin-Walled Structures, 103 (2016) 45-61.

[39] J.N. Reddy, Mechanics of laminated composite plates and shells: theory and analysis, CRC press, 2004.

[40] M. Baruch, J. Arbocz, G. Zhang, Laminated conical shells-considerations for the variations of the stiffness coefficients, in: 35th Structures, Structural Dynamics, and Materials Conference, 1993, pp. 1634.

[41] M.R. Spiegel, Mathematical handbook of formulas and tables, McGraw-Hill, 1999.

HOW TO CITE THIS ARTICLE

M. A. Kouchakzadeh , P. Gholami , M. Shakouri, M. Noghabi, Buckling Analysis of Stiffened Cross-Ply Laminated Conical Shells under Axial Compression Using Generalized Differential Quadrature Method, AUT J. Mech Eng., 5(4) (2021) 535-552.

DOI: 10.22060/ajme.2021.18820.5922